MOLECULAR AND CELLULAR BIOLOGY, Jan. 2009, p. 20–30 Vol. 29, No. 1
0270-7306/09/$08.00+0 doi:10.1128/MCB.00544-08

Glutathione Peroxidase 3 Mediates the Antioxidant Effect of Peroxisome Proliferator-Activated Receptor γ in Human Skeletal Muscle Cells▽†

Sung Soo Chung,[1]§ Min Kim,[1]§ Byoung-Soo Youn,[2] Nam Seok Lee,[2] Ji Woo Park,[2] In Kyu Lee,[3] Yun Sok Lee,[4] Jae Bum Kim,[4] Young Min Cho,[1] Hong Kyu Lee,[1] and Kyong Soo Park[1]*

Department of Internal Medicine, Seoul National University College of Medicine, 28 Yongon-Dong, Chongno-Gu, Seoul 110-744, South Korea[1]; AdipoGen Inc., College of Life Science and Biotechnology, Korea University, Rm 641-B, 1, 5-ka, Anam-dong, Sungbuk-ku, Seoul, South Korea[2]; Department of Internal Medicine, Kyungpook National University, Daegu, South Korea[3]; and Research Center for Functional Cellulomics, Department of Biological Sciences, Seoul National University, Seoul 151-742, South Korea[4]

Received 4 April 2008/Returned for modification 7 May 2008/Accepted 10 October 2008

Oxidative stress plays an important role in the pathogenesis of insulin resistance and type 2 diabetes mellitus and in diabetic vascular complications. Thiazolidinediones (TZDs), a class of peroxisome proliferator-activated receptor γ (PPARγ) agonists, improve insulin sensitivity and are currently used for the treatment of type 2 diabetes mellitus. Here, we show that TZD prevents oxidative stress-induced insulin resistance in human skeletal muscle cells, as indicated by the increase in insulin-stimulated glucose uptake and insulin signaling. Importantly, TZD-mediated activation of PPARγ induces gene expression of glutathione peroxidase 3 (GPx3), which reduces extracellular H_2O_2 levels causing insulin resistance in skeletal muscle cells. Inhibition of GPx3 expression prevents the antioxidant effects of TZDs on insulin action in oxidative stress-induced insulin-resistant cells, suggesting that GPx3 is required for the regulation of PPARγ-mediated antioxidant effects. Furthermore, reduced plasma GPx3 levels were found in patients with type 2 diabetes mellitus and in *db*/*db*/DIO mice. Collectively, these results suggest that the antioxidant effect of PPARγ is exclusively mediated by GPx3 and further imply that GPx3 may be a therapeutic target for insulin resistance and diabetes mellitus.

It is generally accepted that oxidative stress plays a key role in the pathogenesis of diabetes mellitus (DM) and its vascular complications (6, 7, 12, 14, 18, 49). Markers of oxidative stress were shown to be elevated in a diabetic animal model and in patients with DM (40, 43). In addition to the increased production of reactive oxygen species (ROS) in DM, the antioxidant capacity is decreased, and oxidative stress is associated with obesity and insulin resistance (4, 15, 21, 26, 47). Therefore, treatment with antioxidants or overexpression of antioxidant enzymes can, at least partially, prevent oxidative stress-induced insulin resistance (20, 24, 26, 36).

Peroxisome proliferator-activated receptor γ (PPARγ) is a member of the superfamily of nuclear receptors. PPARγ heterodimerizes with retinoid X receptor α (RXRα) and binds to a specific DNA sequence called peroxisome proliferator response element (PPRE). PPARγ is activated when specific ligands bind to the ligand-binding domain. Thiazolidinediones (TZDs), such as troglitazone, rosiglitazone, and pioglitazone, are well-known PPARγ ligands and have been used for the treatment of diabetes. PPARγ is most abundantly expressed in adipose tissues and plays a key role in adipocyte differentiation (42, 46). Since the expression level of PPARγ in muscle is low, the effect of PPARγ ligands on insulin sensitivity in muscle has been explained by the connection between adipose tissue and muscle: activation of PPARγ in adipose tissue decreases the plasma fatty acid levels and modulates the expression of adipokines that contribute to improving insulin resistance in muscle (13). However, the direct role of PPARγ on insulin sensitivity in muscle has been demonstrated in a muscle-specific PPARγ-knockout mouse model (23). Several reports have demonstrated that TZDs, being used to improve insulin sensitivity, also have antioxidant effects; however, little is known regarding the mechanism involved in the antioxidant effect of TZDs (9, 26, 32).

Glutathione peroxidases (GPxs) are members of the family of antioxidant enzymes that scavenge hydrogen peroxide in the presence of reduced glutathione, and seven isoforms having different substrate specificities and tissue distribution have been identified (5, 11, 44). GPx is a selenium-dependent enzyme that contains a selenium atom incorporated within the selenocysteine residue (30). GPx3, also called plasma GPx, is an extracellular enzyme that catalyzes organic hydroperoxides and lipid hydroperoxides as well as hydrogen peroxide (35, 51). GPx3 is highly expressed in the kidney; however, GPx3 mRNA is also found in the lung, heart, liver, eyes, and white adipose tissue (8, 37, 39, 52).

In this study, in order to examine the antioxidant effects of TZDs, human muscle cells were exposed to H_2O_2 that was being generated continuously from glucose oxidase and glucose in the medium. Destruction of insulin signaling by treatment with H_2O_2 or glucose oxidase in vascular smooth muscle cells and adipocytes has been reported (16, 45). Here, we show that high levels of H_2O_2 destroy the insulin signaling pathway, and TZDs prevent H_2O_2-induced insulin resistance in human skeletal muscle cells. This study also provides evidence that PPARγ directly regulates the expression of a gene coding for

* Corresponding author. Mailing address: Department of Internal Medicine, Seoul National University College of Medicine, 28 Yongon-dong, Chongno-gu, Seoul 110-744, South Korea. Phone: 82-2-2072-2946. Fax: 82-2-3676-8309. E-mail: kspark@snu.ac.kr.

† Supplemental material for this article may be found at http://mcb.asm.org/.

§ These two authors contributed equally to this work.

▽ Published ahead of print on 20 October 2008.

an antioxidant enzyme, namely, GPx3, and the antioxidant effect of TZDs in human skeletal muscle cells is mediated mainly by GPx3.

MATERIALS AND METHODS

Plasmids, adenovirus, and antibodies. A DNA fragment from −2,294 bp to +53 bp (from the transcription start site) of the human GPx3 gene was cloned into the region upstream of the luciferase gene of the pGL2-basic vector (Promega, Madison, WI) to generate hGPx3 (−2294) Luc. Further, hGPx3 (−809) Luc was constructed by inserting the promoter fragment, −809/+53 bp, into the pGL2-basic vector. DNA fragments containing two copies of hGPx3 (−2186) PPRE (TAGACCACCAGGGCTGGGATTAAGGTG [PPRE is underlined]) or the PPRE mutant sequence (TAGACCACCAGGGCTGcctaatAGGTG [mutated sequences are in lowercase]) were inserted into the region upstream of the simian virus 40 (SV40) promoter of the pGL2 promoter (Promega, Madison, WI), and the resulting constructs were named pGL2P (−2186) PPRE and pGL2P (−2186) PPREmt, respectively. Adenoviruses expressing PPARγ (Ad-PPARγ) and β-galactosidase (Ad-βGal) were constructed as described previously (25). Adenoviruses expressing hGPx3 (Ad-GPx3) were constructed by insertion of the hGPx3 gene (+1/+1,539 bp) containing the coding region and the 3′ untranslated region of the GPx3 gene into pAd Treck-CMV. The 3′ untranslated region of the GPx3 gene has been reported to be important for production of the full-size protein containing the selenocysteine residue (3). The control virus generated from pAdYCII expresses green fluorescent protein (Ad-GFP). Antibodies against GFP, PPARγ, p38, IKKα/β, and insulin receptor substrate 1 (IRS-1) were purchased from Santa Cruz Biotech, Santa Cruz, CA. The following antibodies were used: antibody against pIRS-1 (Y612) (Biosource, Camarillo, CA); antibodies against pAkt (Ser473), Akt, pIKKα/β, Jun N-terminal kinase (JNK), Erk1/2, and pSer307 IRS (Cell Signaling Technology, Danvers, MA); antibodies against pJNK, p-p38, and p-pErk1/2 (Promega, Madison, WI); and the antibody against GPx3 (Adipogen, Seoul, Korea).

Cell culture and animals. Human muscle tissue was obtained by biopsy of healthy nondiabetic subjects and was immediately dissociated according to previously described methods (22). Satellite cells from the dissociated muscle were grown in skeletal muscle basal medium supplemented with 2% fetal bovine serum (FBS) and singleQuots skeletal muscle growth medium without insulin (Cambrex, Walkersville, MD). When the cells reached confluence, they were maintained in α modified Eagle's medium supplemented with 2% FBS (Welgene, Daegu, Korea) and insulin to induce cell fusion. C2C12 myoblasts were cultured in Dulbecco's modified Eagle's medium (DMEM) supplemented with 10% FBS, and differentiation was induced by changing the medium to DMEM with 2% horse serum (38). COS-7 cells were cultured in DMEM supplemented with 10% FBS. C57BLKSJ/db/db mice and their littermate C57BL/6J mice were used for these experiments (SCL, Japan). Nine-week-old male mice were divided into two groups, i.e., those fed on normal chow ($n = 5$) and those fed on a high-fat diet ($n = 5$). In the latter case, the mice were exposed to a high-fat diet (60% calories from fat; Research Diet, New Brunswick, NJ) for 20 days. Mice belonging to the high-fat diet group ($n = 5$) were treated with rosiglitazone (30 mg/kg of body weight/day; GlaxoSmithKline) for an additional 8 days. The study animals comprised the following: normally fed mice (body weight, 25.9 ± 0.9 g; blood glucose level, 147.0 ± 13.9 mg/dl), high-fat-fed mice (body weight, 31.0 ± 1.5 g; blood glucose level, 213.6 ± 11.2 mg/dl), and high-fat/rosiglitazone-treated mice (body weight, 28.7 ± 0.6 g; blood glucose level, 155.6 ± 10.8 mg/dl). The animals were handled in compliance with the Guidelines for Experimental Animal Research from the Laboratory for Experimental Animal Research, Clinical Research Institute, Seoul National University Hospital.

Measurement of glucose uptake in human skeletal muscle cells. Human muscle cells were differentiated and treated with PPARγ agonists (10 μM) for 48 h, and then 100 mU/ml glucose oxidase (Sigma-Aldrich, St. Louis, MO) was added to the medium for 3 h before the addition of insulin. Glucose oxidase oxidizes β-D-glucose to D-gluconolactone and H_2O_2. After washing with salt-HEPES buffer (130 mM NaCl, 4.7 mM KCl, 1.25 mM $CaCl_2$, 1.2 mM $MgSO_4$, 2.5 mM NaH_2PO_4, and 10 mM HEPES), 0.2 μCi of [^{3}H]deoxyglucose was added into the salt-HEPES buffer for 15 min. Glucose uptake was stopped by aspiration of the buffer and washing the cells five times with cold phosphate-buffered saline (PBS). The cells were lysed with 0.5 N NaOH and neutralized by HCl, followed by liquid scintillation counting in a beta counter. For normalization, total protein was measured by the Bradford assay.

Western blot analysis. Cell lysates (20 μg of protein) were separated on an sodium dodecyl sulfate (SDS)-polyacrylamide gel. Proteins on the SDS-polyacrylamide gel were transferred onto a nitrocellulose membrane. Blocking was performed using 5% skim milk, and primary antibody in 0.1% Tween 20–Tris-buffered saline was then added. Hybridized primary antibodies were detected using a horseradish peroxidase-conjugated species-specific immunoglobulin G antibody. The bands were visualized by enhanced chemiluminescence (Pierce, Rockford, IL).

Northern blot analysis. Total RNAs were isolated by using the TRIzol reagent kit (Invitrogen) or RNeasy minikit (Qiagen, Hilden, Germany) according to the manufacturer's instructions. The RNAs (20 μg) were separated by electrophoresis and transferred onto a Nytran membrane (NY 13-N; Schleicher & Schuell, Stanford, ME). The membranes were prehybridized in QuickHyb hybridization solution (Stratagene), hybridized with [α-^{32}P]dATP-labeled cDNA fragments of GPx3 or glyceraldehyde-3-phosphate dehydrogenase (GAPDH), and exposed to X-ray films. To prepare RNA from tissues, fresh frozen tissues were ground in a mortar chilled with liquid nitrogen, the powdered tissues were added to TRIzol (Invitrogen), and total RNA was prepared.

Treatment with glucose oxidase and measurement of H_2O_2. Human muscle cells were differentiated, and the medium was then changed to phenol red-free minimum essential medium (Invitrogen) supplemented with 2% FBS. Cells were treated with PPARγ agonists, adenovirus, or short interfering RNA (siRNA) for 48 h, and then glucose oxidase was added to the medium. The amount of H_2O_2 in the medium was measured using a method described previously (36). Absorbance was measured at 491 nm (VersaMax; Molecular Devices, Sunnyvale, CA) using *t*-butyl hydroperoxide as the standard. *N*-Acetylcysteine (NAC; 10 mM; Sigma-Aldrich) and recombinant catalase (1,600 mU/ml; Sigma-Aldrich) treatment was performed prior to the addition of glucose oxidase.

Determination of intracellular ROS. Human muscle cells were treated with glucose oxidase and were washed three times with PBS. The cells were incubated with 10 μg/ml 2′,7′-dichlorohydrofluorescein diacetate (DCF-DA; Invitrogen) in PBS for 5 min and were washed. Fluorescence was detected by excitation at 485 nm and emission at 535 nm using a Victor 3 instrument (Perkin-Elmer, Boston, MA).

Microarray analysis. Human skeletal muscle cells were differentiated and treated with troglitazone (10 μM) or dimethyl sulfoxide (DMSO) (control) for 48 h. Total RNAs were isolated by using the RNeasy midiprep kit (Qiagen, Hilden, Germany) and subjected to microarray analysis (Human Oligo 10K chip; Macrogen, Seoul, South Korea).

Transient-transfection and reporter assays. COS-7 cells were transiently transfected with luciferase reporter vectors containing different lengths of the human GPx3 promoter (0.3 μg), pcDNA-PPARγ (0.05 μg), pFLAG-RXRα (0.05 μg), and pCMV-βGal (0.05 μg) using Lipofectamine Plus reagent (Invitrogen). COS-7 cells were transfected with 0.15 μg of the reporter vectors [pGL2P, pGL2P (−2186) PPRE, or pGL2P (−2186) PPREmt], pcDNA-PPARγ (0.03 μg), pFLAG-RXRα (0.03 μg), and pCMV-βGal (0.05 μg). Troglitazone (10 μM) and 9-*cis*-retinoic acid (1 μM) were added 3 h after transfection, and the cells were incubated for 40 h. The cells were harvested for the analysis of luciferase activity (Promega), and the relative transfection efficiency was determined by measuring β-galactosidase activity.

Electrophoretic mobility shift assay (EMSA). Oligonucleotides for hGPX3 (−2186) PPRE (−2195/−2169 bp) (TAGACCACCAGGGCTGGGATTAAG GTG, upper strand) and the (−2186) PPRE mutant (TAGACCACCAGGGC TGcctaatAGGTG, upper strand) were used as a probe or competitor. The sequence of consensus PPRE competitor was CAGGGGACCAGGACAAAG GTCACGTTGCGGA. The probes were labeled with [α-^{32}P]dATP using Klenow polymerase (Ambion, Austin, TX), and the labeled probe (25,000 cpm) was incubated with the nuclear extracts of the human skeletal muscle cells treated with troglitazone or rosiglitazone for 48 h in 10 mM HEPES (pH 7.9) containing 50 mM KCl, 0.1 mM EDTA, 0.25 mM dithiothreitol (DTT), 0.1 mg/ml poly(dI-dC), 0.01% Nonidet P-40, and 10% glycerol at room temperature for 10 min. Competitors were added at 50- or 100-fold molar excesses to the labeled probe. The DNA-protein complexes were separated on 5% polyacrylamide gels and were detected by autoradiography.

Chromatin immunoprecipitation (ChIP). The differentiated human skeletal muscle cells were treated with rosiglitazone for 48 h. The cells were cross-linked in 1% formaldehyde at 37°C for 10 min and were resuspended in buffer 1 (100 mM Tris-HCl, pH 9.4; 10 mM DTT; protease inhibitors). The nuclei were isolated in buffer 2 (10 mM Tris-HCl, pH 8.0; 0.25% X-100; 0.5% NP-40; 10 mM EDTA; 0.5 mM EGTA; 1 mM DTT; protease inhibitors) by centrifugation. Nuclear extracts were prepared in buffer 3 (10 mM Tris-HCl, pH 8.0; 1 mM EDTA; 0.5 mM EGTA; 1 mM DTT; protease inhibitors) and sonicated. The nuclear extracts (500 μl) were then incubated overnight with anti-PPARγ antibody (3 μg), salmon sperm DNA (2 μg), and protein G-Sepharose (20 μl) at 4°C in radioimmunoprecipitation assay buffer. After being washed several times, the immunoprecipitates were eluted using an elution buffer (1% SDS and 0.1 M

$NaHCO_3$). To reverse the cross-linking, the immunoprecipitates were incubated in 200 mM NaCl, and the DNA was purified by phenol-chloroform and ethanol precipitation. The following primers were used for PCR: 5′-GCCCATGGGAA GTAGGATGT-3′ and 5′-TGGGATTATAGGCACCACCA-3′ (−7234 PPRE candidate), 5′-TGTGACCAGCCCCTAACAAA-3′ and 5′-GGAGGACTCAC AGAACTCAGCA-3′ (−5442 PPRE candidate), 5′-CAGCACAGATCAGTTT GTACTAGCC-3′ and 5′-GAAAACCTTAGCGGCTTTCCT-3′ (−4651 PPRE candidate), and 5′-AGCAATCCAGGGGTAGCATC-3′ and 5′-CCCTGCTCT CAAAGGTGTTTC-3′ (−2186 PPRE candidate).

Transfection of siRNA. The siRNAs of hGPx3 and hPPARγ were purchased from Dharmacon, Lafayette, CO. The siRNA of the negative control (NS) was purchased from Bioneer, Seoul, South Korea. The siRNA (On-Target*plus* Smart pool or NS; 100 nM) was incubated with Lipofectamine 2000 (Invitrogen) in 100 μl serum-free medium for 15 min. The siRNA-Lipofectamine 2000 complex was then added to the cells in 400 μl of serum-containing medium and maintained for 3 days.

GPx3 ELISA. The gene encoding human GPx3 whose internal selenocysteine had been mutated to cysteine was amplified by PCR. For producing the recombinant GPx3 protein in human embryonic kidney (HEK) 293 cells, the DNA sequence encoding hGPx3 (Gln21 to Lys226) was tagged with FLAG at the C terminus, and its secretion was facilitated using PAI-1 leader peptide. Polyclonal antibody was prepared from rabbits according to the general protocols. Immunoglobulin fractions were prepared from serum. A sandwich enzyme-linked immunosorbent assay (ELISA) format that used FLAG-tagged GPx3 was designed. The extracellular GPx3 protein levels in the medium were measured by using ELISA kits. The plasma GPx3 concentration was also measured in 49 subjects with type 2 DM and in age- and sex-matched subjects with normal glucose tolerance (NGT; $n = 57$) and impaired glucose tolerance (IGT; $n = 48$) by using ELISA kits. The status of NGT, IGT, and DM was determined on performing the 75-g oral glucose tolerance test according to the diagnostic criteria of the American Diabetes Association (1).

Statistical analysis. Statistical analysis was performed using GraphPad InStat (version 3.05; GraphPad Software Inc.). The differences between the means were assessed by Student's *t* test or one-way analysis of variance. The data have been expressed as the means ± standard errors of the means. A P value of less than 0.05 was considered to denote a statistically significant difference.

RESULTS

Treatment with TZDs overcomes the effect of ROS on insulin signaling and glucose transport in human skeletal muscle cells. To investigate whether TZD modulates the effect of ROS on the insulin signaling pathway in skeletal muscle cells, we prepared human skeletal muscle cells and incubated them with glucose oxidase, which continuously produces H_2O_2 using glucose as a substrate. When the cells were incubated with glucose oxidase (100 mU/ml) for 3.5 h in the absence of troglitazone, insulin-stimulated tyrosine phosphorylation of IRS-1 and phosphorylation at serine 473 of Akt/PKB were completely inhibited (Fig. 1A). This was similar to the result found by other researchers in experiments involving 3T3-L1 adipocytes (45). Pretreatment with troglitazone, a member of the TZDs, for 48 h completely restored insulin-induced activation of IRS-1 and Akt in the presence of glucose oxidase (Fig. 1A). Next, we tested the effect of troglitazone on the glucose uptake in human skeletal muscle cells. When the cells were incubated with a high level of H_2O_2 generated by glucose oxidase, glucose uptake was significantly decreased in both the basal and insulin-stimulated states (Fig. 1B). Pretreatment with troglitazone, however, increased the glucose uptake by three- to fourfold both in the absence and in the presence of insulin and completely ameliorated the effect of H_2O_2.

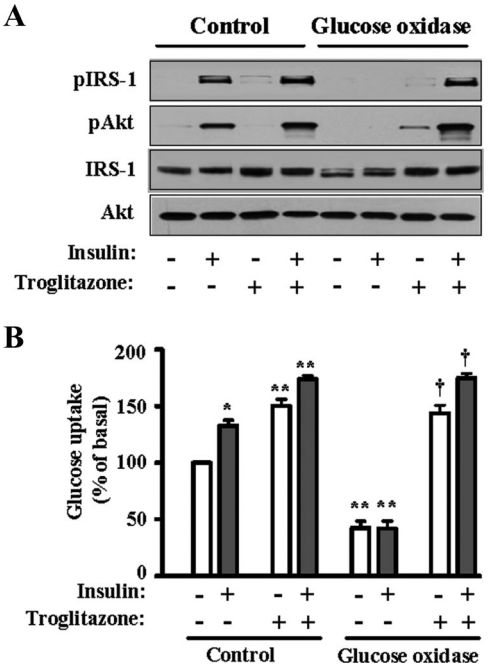

FIG. 1. Effect of troglitazone on the insulin signaling pathway and impairment of glucose uptake by H_2O_2 in human skeletal muscle cells. (A) Human skeletal muscle cells were prepared and differentiated as described in Materials and Methods. The cells were treated with glucose oxidase (100 mU/ml) for 3 h and then with insulin (100 nM) for 30 min. For troglitazone treatment, the cells were pretreated with troglitazone for 48 h and then with glucose oxidase and insulin. The cells were harvested, and 20 μg of proteins was subjected to SDS-polyacrylamide gel electrophoresis and Western blot analysis. (B) Glucose uptake was measured as described in Materials and Methods. The cells were treated with glucose oxidase (100 mU/ml) for 3 h and then incubated with or without insulin (100 nM) for 30 min. For troglitazone treatment, the cells were pretreated with troglitazone for 48 h and then with glucose oxidase and insulin. The glucose uptake of untreated cells was set as 100, and the other values were expressed relative to it. The bar graph represents the mean ± standard error of four independent experiments; *, $P < 0.01$ versus the basal value of control cells not treated with troglitazone; **, $P < 0.01$ versus the corresponding value of control cells not treated with troglitazone, †, $P < 0.01$ versus the corresponding value of cells treated with glucose oxidase but not with TZDs.

PPARγ is involved in the antioxidant effect of TZDs. To determine whether the protective effect of TZDs against ROS was PPARγ dependent, a PPARγ antagonist, GW9662, was added to the medium. The antioxidant effect of troglitazone almost disappeared in the presence of GW9662 (Fig. 2A). A similar effect was observed when PPARγ expression was knocked down by transfection with PPARγ siRNAs: the antioxidant effect of rosiglitazone was completely abolished by knockdown of PPARγ (Fig. 2B). These results suggested that the antioxidant effect of TZDs was PPARγ dependent. When the cells were treated with troglitazone for 3 h instead of 48 h, insulin-induced phosphorylation of IRS-1 and Akt was not observed in the presence of glucose oxidase (Fig. 2C). In addition, the antioxidant effect of troglitazone disappeared when the culture medium was replaced with fresh medium before treatment with glucose oxidase (Fig. 2D). To summarize these results, an extracellular protein was involved in the antioxidant effect of TZDs, and the expression of this protein was induced by PPARγ activation.

TZDs decrease extracellular H_2O_2 levels. Since the data in Fig. 2 showed that an extracellular protein was involved in the

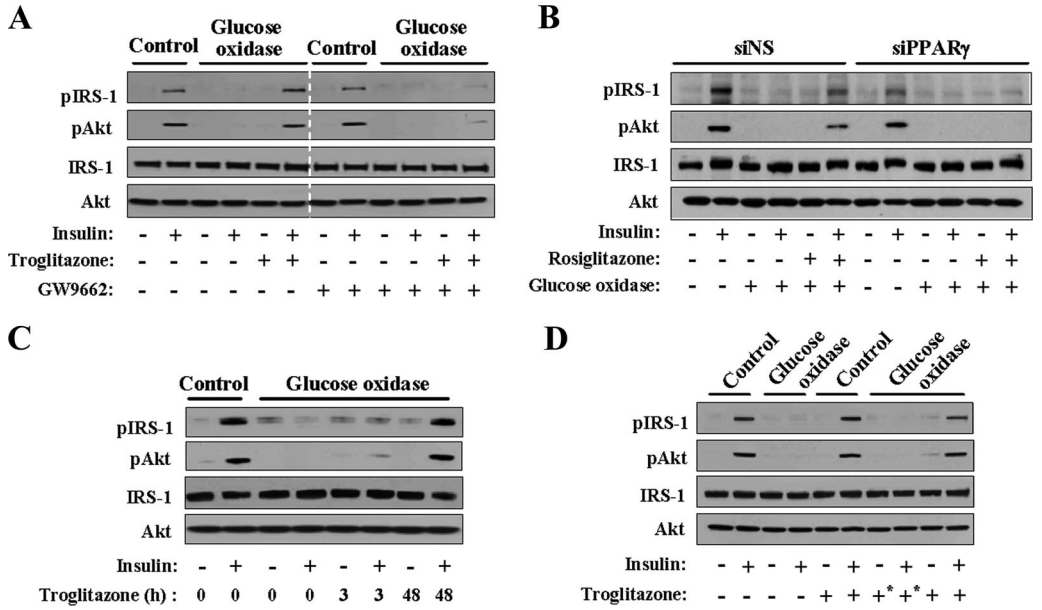

FIG. 2. Antioxidant effects of TZDs are PPARγ dependent. Western blot analysis. For each figure, at least three independent experiments were performed, and similar results were obtained. (A) Cells were treated with troglitazone in the presence or absence of GW9662 (10 μM), a PPARγ antagonist, for 48 h and then with glucose oxidase for 3 h. (B) The cells were transfected with siRNAs of PPARγ (siPPARγ) or control (siNS) using Lipofectamine 2000. The cells were treated with rosiglitazone 24 h after siRNA transfection and were incubated for an additional 48 h. (C) The cells were treated with troglitazone for 3 h or 48 h, and then glucose oxidase was added. (D) The cells were treated with troglitazone for 48 h, and a set of cells (+*) was washed with PBS and incubated with fresh medium prior to the addition of glucose oxidase.

antioxidant effect of TZDs, we examined the effect of TZDs on the level of extracellular H_2O_2 generated by glucose oxidase in the culture medium of human skeletal muscle cells. When the cells were treated with troglitazone for 48 h, the extracellular H_2O_2 level decreased significantly (Fig. 3A). However, when the cells were incubated with troglitazone for less than 6 h, the H_2O_2 level did not decrease, and the longer the duration of troglitazone treatment, the lower the H_2O_2 levels that were elicited (Fig. 3B). Similar results were obtained when rosiglitazone was used (data not shown). Furthermore, each of the three TZDs, namely, troglitazone, rosiglitazone, and pioglitazone, reduced the H_2O_2 levels in the medium (Fig. 3C). To test whether gene expression was involved in this effect, cycloheximide, a protein synthesis inhibitor (10 μg/ml), was added to the cells simultaneously with TZDs. Treatment with cycloheximide completely inhibited the effect of troglitazone and rosiglitazone (Fig. 3D). This result showed that the antioxidant effect of TZDs is completely dependent on the synthesis of a protein.

TZDs decrease intracellular ROS levels. Next, we directly examined the level of intracellular ROS in the presence of glucose oxidase and TZDs. Incubation with glucose oxidase significantly increased the intracellular ROS concentration, which was detected by DCF fluorescence, and treatment with TZDs decreased the intracellular ROS levels to almost the basal levels (Fig. 3E). The effects of the increase in the intracellular ROS levels by glucose oxidase treatment were investigated in greater detail: activation of ROS-responsive Ser/Thr kinases, such as JNK, p38, and Erk1/2, was examined. Phosphorylation of JNK, p38, and Erk1/2 was increased in line with the increase in the intracellular ROS levels by glucose oxidase, and TZDs suppressed the activation of these kinases (Fig. 3F). Similar results were obtained from IKK phosphorylation and phosphorylation at Ser307 of IRS-1 (Fig. 3F). These results clearly showed that the extracellular H_2O_2 produced by glucose oxidase entered into the cells and increased the intracellular ROS levels and that TZDs decreased the intracellular ROS levels by downregulation of the extracellular H_2O_2.

Effect of PPARγ activation on the expression of GPx3. To determine the gene whose expression is induced by PPARγ activation and which is involved in the antioxidant effect of TZDs, we used microarray analysis to examine the expression patterns of many genes in human skeletal muscle cells treated with troglitazone. Several genes, such as CD 36, adipose differentiation-related protein, and apolipoprotein E, which are known to be targets of PPARγ, were induced by PPARγ activation (see Fig. S1 in the supplemental material). Interestingly, the expression of GPx3 was dramatically increased by PPARγ activation; however, the expression of a number of genes encoding other antioxidant enzymes was hardly changed (see Fig. S1 in the supplemental material). To confirm the findings of the microarray analysis, the mRNA level of GPx3 was determined by Northern blot analysis. The GPx3 mRNA level was dramatically increased by troglitazone and was further increased by PPARγ overexpression in the cultured human skeletal muscle cells (Fig. 4A). In contrast, the GPx1 mRNA level was not increased by troglitazone, suggesting that this effect is specific to the GPx3 gene and cannot be generalized to other members of the GPx family. While rosiglitazone, pioglitazone, and troglitazone increased the mRNA level of GPx3, wy14643—a PPARα ligand—did not increase the GPx3 mRNA level (Fig. 4B). Expression of the GPx3 gene was gradually increased by rosiglitazone up to 48 h (Fig. 4C). Similar results were obtained with troglitazone and pioglitazone (data

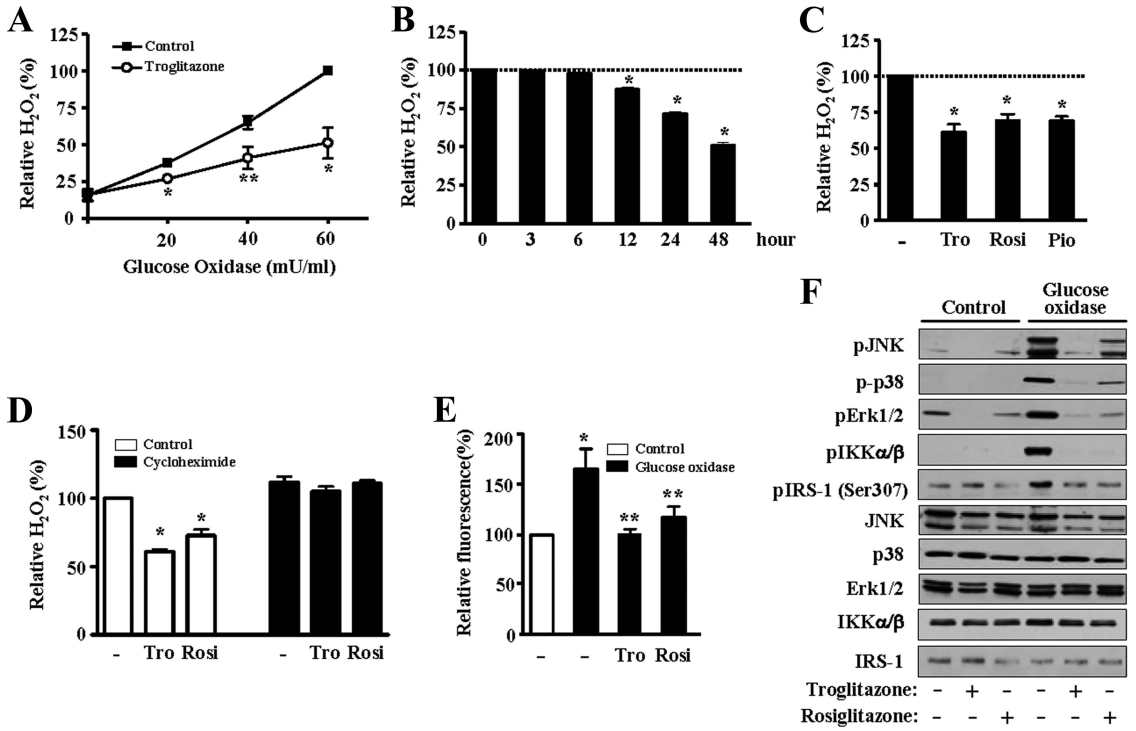

FIG. 3. Effect of TZDs on extracellular H_2O_2 concentration. (A) The amount of H_2O_2 in the medium was measured after the human skeletal muscle cells were treated with troglitazone for 48 h and different doses of glucose oxidase for 1 h. The graph represents the mean ± standard error of three independent experiments. *, $P < 0.01$; **, $P < 0.05$ (versus the control). (B) Cells were treated with troglitazone for the indicated periods of time and with glucose oxidase for 1 h. The bar graph represents the mean ± standard error of three independent experiments. *, $P < 0.01$ versus the H_2O_2 concentration at 0 h. (C) Cells were treated with various PPARγ agonists, namely, troglitazone, rosiglitazone, or pioglitazone, for 48 h and with glucose oxidase for 1 h ($n = 5$); *, $P < 0.01$ versus the value of control cells. (D) Cycloheximide (10 μg/ml) was added to the cells along with TZDs ($n = 5$). *, $P < 0.01$ versus the value of control cells. (E) After the cells were treated with glucose oxidase for 1 h in the absence or presence of TZDs (48 h), the intracellular ROS level was detected by DCF-DA as described in Materials and Methods. The value of cells not treated with glucose oxidase was set to 100, and the other values were presented in relation to that value. The bar graph shows the mean ± standard errors of four independent experiments. *, $P < 0.05$ versus the value of control cells not treated with glucose oxidase; **, $P < 0.05$ versus the value of cells treated with glucose oxidase but not with TZDs. (F) Cells treated with troglitazone or rosiglitazone for 48 h and then treated with glucose oxidase for 1 h. The cells were harvested, and the proteins were subjected to Western blot analysis using antibodies against phospho-JNK, p38, Erk1/2, IKKα/β, and Ser307 IRS-1 or total JNK, p38, Erk1/2, IKKα/β, and IRS-1.

not shown). Since PPARγ and RXRα bind to a target DNA sequence (PPRE) as a heterodimer, we tested the effect of an RXRα agonist, 9-*cis*-retinoic acid, on the expression of GPx3. A synergistic increase in GPx3 mRNA expression was detected after simultaneous treatment with troglitazone and 9-*cis*-retinoic acid (Fig. 4D). When PPARγ was activated by TZDs in mouse C2C12 myotubes, GPx3 expression was also increased (data not shown), indicating that the regulation of the GPx3 gene by PPARγ is conserved between species. In addition to the determination of GPx3 at the mRNA level, the increase in GPx3 by PPARγ activation was also determined at the protein level by ELISA, and the result showed that extracellular GPx3 protein level was increased by troglitazone (Fig. 4E).

Identification of a PPRE in the human GPx3 promoter. To investigate whether PPARγ directly affects GPx3 promoter activity, DNA fragments representing the human GPx3 promoter were linked to the luciferase reporter gene. Activation of PPARγ and RXRα increased the promoter activity of hGPx3 (−2294) Luc by approximately 3.5-fold in COS7 cells (Fig. 5A). In contrast, PPARγ activation had little effect on the activity of a smaller construct, hGPx3 (−809) Luc. A DNA sequence similar to the consensus PPRE was found at −2186/−2174 bp of the human GPx3 gene. We also performed ChIP: four regions in the GPx3 promoter presumed to contain PPRE candidates (−7234, −5442, −4651, and −2186 PPRE candidates) were tested. Among these candidates, only the PPRE candidate at −2186 in the hGPx3 promoter could be immunoprecipitated with the anti-PPARγ antibody (Fig. 5B). In our study, the binding activity of PPARγ was not changed by rosiglitazone, and similar phenomena have been reported by other researchers (10, 19). EMSA with in vitro-translated PPARγ and RXRα showed that they specifically bound to hGPx3 (−2186) PPRE (data not shown). In addition, EMSA using nuclear extracts of human skeletal muscle cells and competitors also proved that this sequence is a specific PPRE (Fig. 5C). An oligomer containing a mutated sequence in hGPx3 (−2186) PPRE did not compete with the probe (lanes 5 and 6), and an oligomer representing the consensus PPRE competed well with the hGPx3 PPRE probe (lanes 7 and 8). To further investigate the function of this sequence as a PPRE, a DNA fragment representing two copies of this sequence was inserted into the region upstream of the SV promoter in the pGL2-pro vector. PPARγ activation increased the promoter activity of GPx3 (−2186) PPRE Luc (Fig. 5D). In contrast, when the

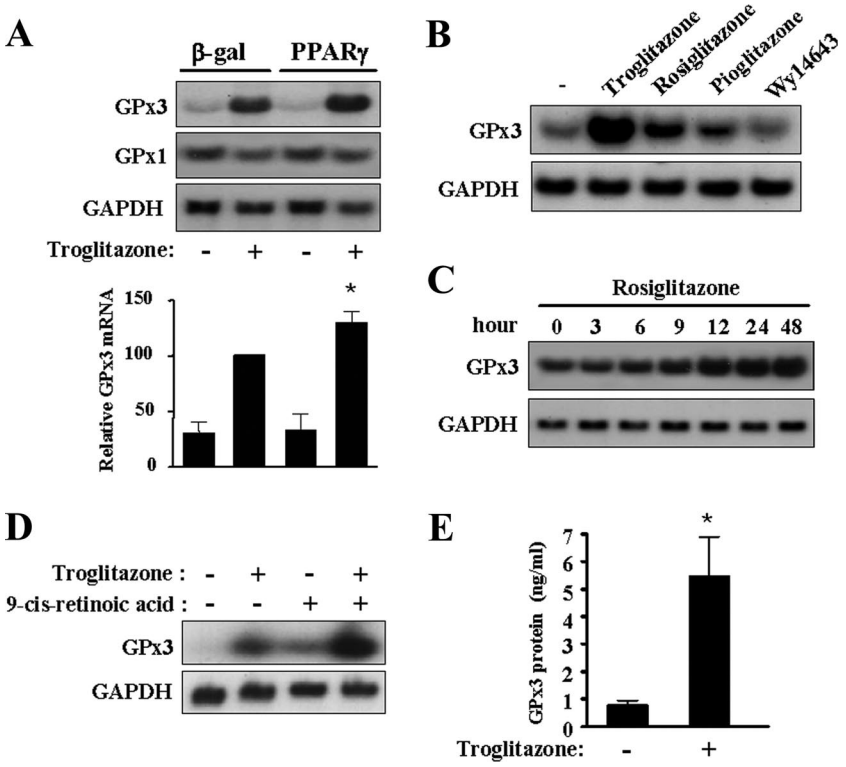

FIG. 4. TZDs induce GPx3 expression in human skeletal muscle cells. For Northern blot analysis in panels A to D, at least three independent experiments were performed, and similar results were obtained. (A) Human skeletal muscle cells were infected with Ad-βGal or Ad-PPARγ and then treated with troglitazone for 48 h. Total RNA was prepared and subjected to Northern blot analysis. The band intensity of GPx3 was normalized to that of GAPDH and presented as a bar graph. The GPx3 mRNA level of Ad-βGal- and troglitazone-treated cells was set as 100, and the other values were represented in relation to it. The graph represents the mean ± standard error of three independent experiments. *, $P < 0.05$ versus the value obtained from cells treated with Ad-βGal and troglitazone. (B) Human skeletal muscle cells were treated with 10 μM of troglitazone, rosiglitazone, pioglitazone, or wy14643 (a PPARα agonist) for 48 h. (C) Human skeletal muscle cells were treated with rosiglitazone for the indicated periods of time. (D) Cells were treated with troglitazone (10 μM) and 9-*cis*-retinoic acid (1 μM) for 48 h. (E) After treatment with troglitazone for 48 h, extracellular GPx3 was determined by ELISA. The bar graph shows the mean ± standard error of four independent experiments. *, $P < 0.01$.

PPRE sequence was mutated, the effect of PPARγ activation on the transcriptional activity was totally abolished. These results suggested that PPARγ directly regulates the expression of GPx3 by binding to the PPRE.

Effect of overexpression of GPx3 on ROS levels. We next tested whether overexpression of GPx3 directly affects the extracellular H_2O_2 concentration and the insulin signaling pathway in skeletal muscle cells. Overexpression of GPx3 by infection with Ad-GPx3 was confirmed on its mRNA (Fig. 6A). While GPx3 expression was increased, the extracellular H_2O_2 concentration was decreased in the presence of glucose oxidase (Fig. 6B). In addition, activation of ROS-responsive factors, such as JNK, p38, and Erk1/2, by glucose oxidase was inhibited by overexpression of GPx3 (Fig. 6C), thereby proving that the increase in the intracellular ROS levels in the presence of glucose oxidase was protected by overexpression of GPx3. Consistent with this result, the insulin signaling pathway was restored almost completely by the overexpression of GPx3 in the presence of glucose oxidase (Fig. 6D).

Role of GPx3 in the antioxidant effect of TZDs. To determine the contribution of GPx3 to the antioxidant effect of TZDs, we knocked down GPx3 gene expression by transfection with GPx3 siRNAs and examined the antioxidant effect of TZDs. Administration of PPARγ siRNA or GPx3 siRNA significantly reduced the level of PPARγ or GPx3 mRNA, respectively (Fig. 7A). In addition, induction of GPx3 expression by TZDs was also repressed by PPARγ siRNA, clearly suggesting that GPx3 expression is regulated by PPARγ. The extracellular H_2O_2 concentration in the presence of TZDs was significantly increased by the suppression of PPARγ or GPx3 expression (Fig. 7B). Consistent with this finding, the antioxidant effect of rosiglitazone observed on the ROS-responsive factors, including JNK, p38, and Erk1/2, was abolished when GPx3 expression was suppressed by specific siRNAs (Fig. 7C). In addition, rosiglitazone could not restore the insulin signaling pathway impaired by glucose oxidase in the presence of GPx3 siRNA (Fig. 7D). A similar effect was observed in the glucose uptake levels: the antioxidant effect of troglitazone was inhibited by knockdown of GPx3 (Fig. 7E). Based on these results, we conclude that GPx3 is a major protein involved in the antioxidative effect of TZDs.

Expression of GPx3 in diabetic patients and animal models. Next, we examined the relationship between GPx3 expression and diabetes. Plasma GPx3 levels in patients with type 2 DM were significantly lower than those in subjects with NGT or IGT (Fig. 8A). The plasma GPx3 protein concentration in *db*/*db* mice was

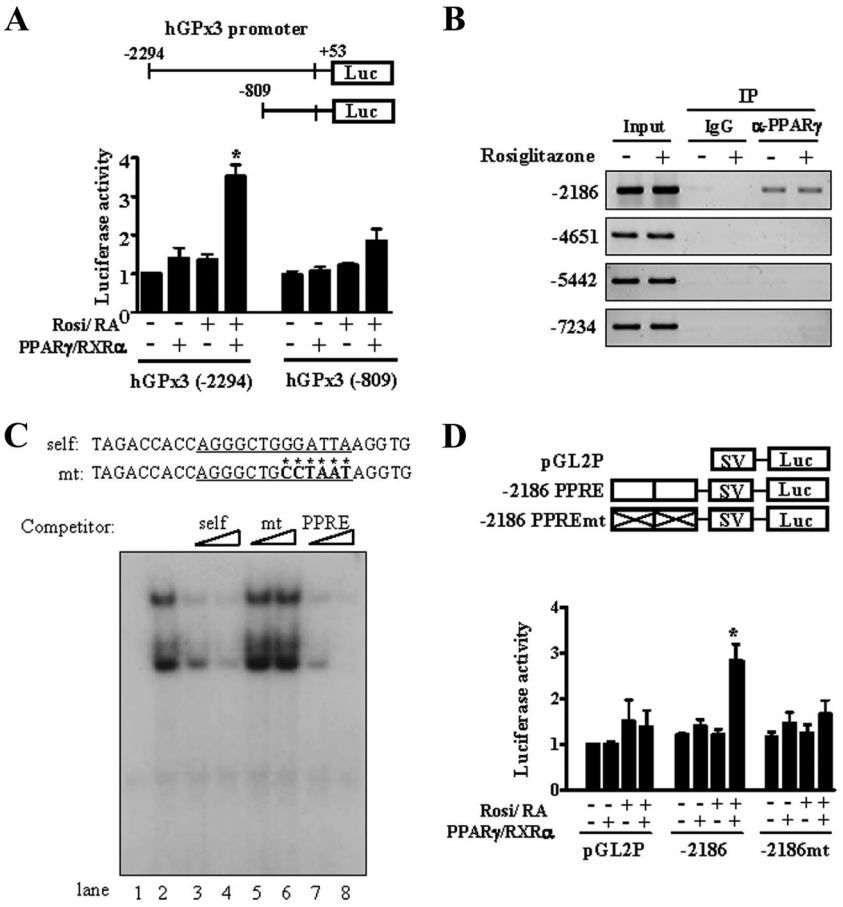

FIG. 5. Identification of a PPRE in the hGPx3 gene. (A) COS-7 cells were transfected with the indicated vectors containing the hGPx3 promoter (hGPx3 (−2294) Luc or hGPx3 (−809) Luc), the expression vectors of PPARγ, RXRα, and β-galactosidase. Rosiglitazone (Rosi) (10 μM) and 9-*cis*-retinoic acid (RA) (1 μM) were added for 48 h. β-Galactosidase activity was used as an internal control to monitor the transfection efficiency. The luciferase activity of hGPx3 (−2294) Luc in the absence of PPARγ/RXRα expression and agonists was set as 1, and other activities were expressed relative to it. The bar graph represents the mean ± standard error of six independent experiments. *, $P < 0.01$ versus the activity of hGPx3 (−2294) Luc without PPARγ/RXRα and their agonists. (B) ChIP was performed on human skeletal muscle cells treated or not treated with rosiglitazone. Immunoprecipitation was performed using control immunoglobulin G or anti-PPARγ antibody (α-PPARγ). PCR was performed using the primers described in Materials and Methods, and 10% of the cell lysates used for immunoprecipitation was used as the input. Similar results were obtained from three independent experiments. (C) EMSA was performed using an oligomer representing hGPx3 PPRE at −2186 as a probe and nuclear extracts of human skeletal muscle cells treated with rosiglitazone. For competition assays, unlabeled oligomers representing the hGPx3 (−2186) PPRE (self) (lanes 3 and 4), PPRE mutant (mt) (lanes 5 and 6), or a consensus PPRE (PPRE) (lanes 7 and 8) were used at a 50- or 100-fold molar excess. Lane 1 shows only the probe, and lane 2 shows the control without the competitor. (D) COS-7 cells were transiently transfected with pGL2P, pGL2P (−2186) PPRE, or pGL2P (−2186) PPREmt, expression vectors of PPARγ and RXRα, and pCMV-β-galactosidase. Luciferase activity was normalized by β-galactosidase activity, the value of pGL2P Luc without any treatment was set as 1, and other activities were expressed in relation to it. The bar graph represents the mean ± standard error of four independent experiments. *, $P < 0.05$ versus the activity of pGL2P (−2186) Luc without PPARγ/RXRα and their agonists.

also lower than that in normal mice (data not shown). In addition, the GPx3 mRNA level was decreased in the skeletal muscles of *db*/*db* mice (Fig. 8B). Further investigation with the high-fat diet model showed that mice fed with the high-fat diet had lower GPx3 expression levels than those fed with the standard chow, and rosiglitazone treatment increased the GPx3 expression levels in the high-fat diet-fed mice (Fig. 8C). These results strongly suggested the existence of a relationship between the GPx3 expression level and diabetes.

DISCUSSION

Oxidative stress has been proposed to play an important role in the pathogenesis of insulin resistance, diabetes, and diabetic vascular complications. ROS activates serine/threonine kinase cascades, such as JNK and mitogen-activated protein kinase cascades, leading to serine phosphorylation of the insulin receptor or IRS-1 and results in impaired insulin signaling (4, 31, 36). In this study, we induced insulin resistance in human skeletal muscle cells by adding glucose oxidase to the culture media. To confirm that the impairment in insulin signaling shown in these experiments was induced by H_2O_2 produced by glucose oxidase, NAC, a well-known antioxidant, was added to the medium. Treatment with NAC led to complete recovery of insulin-induced phosphorylation of IRS-1 and Akt in the presence of glucose oxidase (see Fig. S2 in the supplemental material), suggesting that the H_2O_2 produced by glucose oxidase

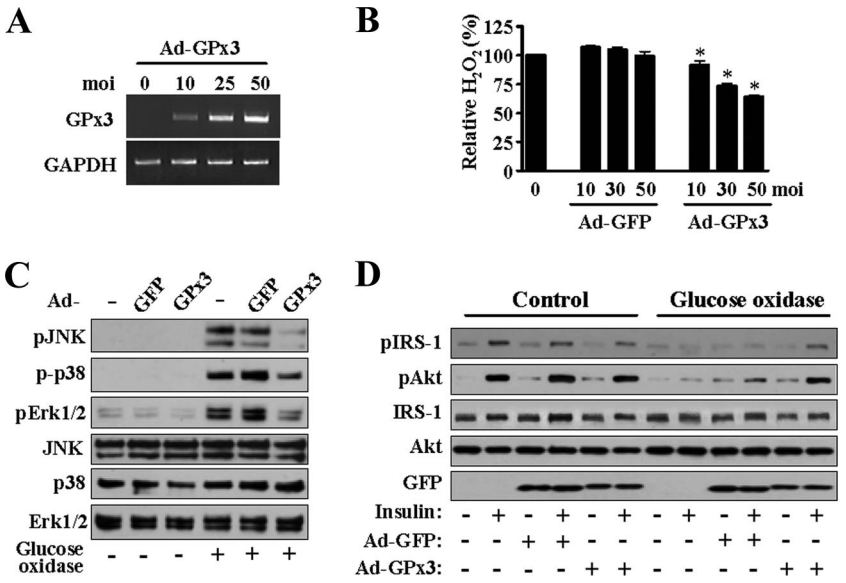

FIG. 6. Effect of GPx3 overexpression on extracellular ROS and insulin resistance induced by glucose oxidase. For each panel, at least three independent experiments were performed. (A) Human skeletal muscle cells were infected with Ad-GPx3 for 48 h. The increase in GPx3 mRNA was determined by reverse transcription-PCR. (B) The cells were infected with Ad-GFP or Ad-GPx3 for 48 h, and the extracellular H_2O_2 concentrations were measured 1 h after incubation with glucose oxidase. The amount of H_2O_2 in the medium of glucose oxidase-treated cells was set as 100, and other values were expressed in relation to it. The bar graph represents the mean ± standard error of three independent experiments. *, $P < 0.01$ versus the value of cells transfected with the same multiplicity of infection (moi) of Ad-GFP. (C) The cells were treated with the adenovirus, i.e., with Ad-GFP (control) or Ad-GPx3, at a multiplicity of infection of 50 for 48 h and then with glucose oxidase for 3 h. The cellular proteins were prepared and subjected to immunoblot analysis. (D) The cells were treated with the adenovirus and glucose oxidase as described for panel C and then with insulin for 30 min. The cellular proteins were prepared and subjected to immunoblot analysis.

interferes with the insulin signaling pathway. The H_2O_2 concentration in the medium reached 1 mM after incubation with glucose oxidase (100 mU/ml) for 3.5 h. This concentration of H_2O_2 is similar to that used in other reports in which insulin resistance was induced in in vitro cell culture systems of HEK 293 and 3T3-L1 adipocytes (21, 45). This concentration may not be physiological; however, the intracellular H_2O_2 concentration would be much lower than the extracellular H_2O_2 concentration because H_2O_2 gradients are established across the plasma membrane despite H_2O_2 being small enough to diffuse directly into the cells (2). We directly detected the increase in intracellular ROS levels and the activation of ROS-responsive Ser/Thr kinases, such as JNK and mitogen-activated protein kinase, by glucose oxidase (Fig. 3E and F). Insulin-induced phosphorylation of IRS-1 and Akt was completely inhibited by H_2O_2 generated by glucose oxidase, and glucose uptake was also impaired in our cell culture system (Fig. 1). We confirmed the antioxidant effect of TZDs in skeletal muscle cells by showing that TZDs restored the insulin signaling pathway and insulin-induced glucose uptake, which were impaired by H_2O_2.

The results shown in Fig. 2 and 3 indicate that an extracellular protein whose expression was induced by TZDs mediated the antioxidant effect of TZDs by reducing the extracellular ROS levels. Therefore, we need to confirm whether addition of an antioxidant protein to the medium can modulate intracellular ROS levels and the insulin signaling pathway by reducing extracellular ROS levels. Recombinant catalase, a well-known antioxidant enzyme, was added to the medium, and its protective effect against glucose oxidase treatment was examined. In the presence of catalase, the glucose oxidase-induced increase in the extracellular and intracellular ROS levels was significantly suppressed (see Fig. S3A and B in the supplemental material), and insulin signaling occurred normally (see Fig. S3C in the supplemental material), suggesting that induction of an extracellular antioxidant protein may modulate the intracellular oxidative status.

Among the antioxidant enzyme genes, a functional PPRE in the rat catalase promoter has been reported (17). However, the microarray analysis results of our study (see Fig. S1 in the supplemental material) showed that GPx3 expression in skeletal muscle cells was significantly increased by TZD treatment, while the expression of the other antioxidant enzyme-encoding genes such as the other GPx family members, Mn superoxide dismutases and catalase, were hardly affected. Therefore, we could hypothesize that in skeletal muscle, the PPARγ-dependent-antioxidant effect of TZDs is exclusively mediated by GPx3. Finally, we observed that GPx3 knockdown by siRNA treatment almost abolished the antioxidant effects of TZDs in the skeletal muscle cells, which strongly supported our hypothesis. We, however, could not exclude the possibility that another mechanism(s) is also involved in the antioxidant effect of TZDs. PPARγ activation has been reported to negatively regulate the expression of NADPH oxidase, resulting in decreased ROS production in endothelial cells (27). Troglitazone has been reported to have a direct antioxidant-scavenging activity on free radicals, unlike other TZDs (9). Eventually, however, we believe that the increased expression of GPx3 is the major mechanism for the antioxidant effect of TZDs in skeletal muscle cells because PPARγ and a secreted protein are important

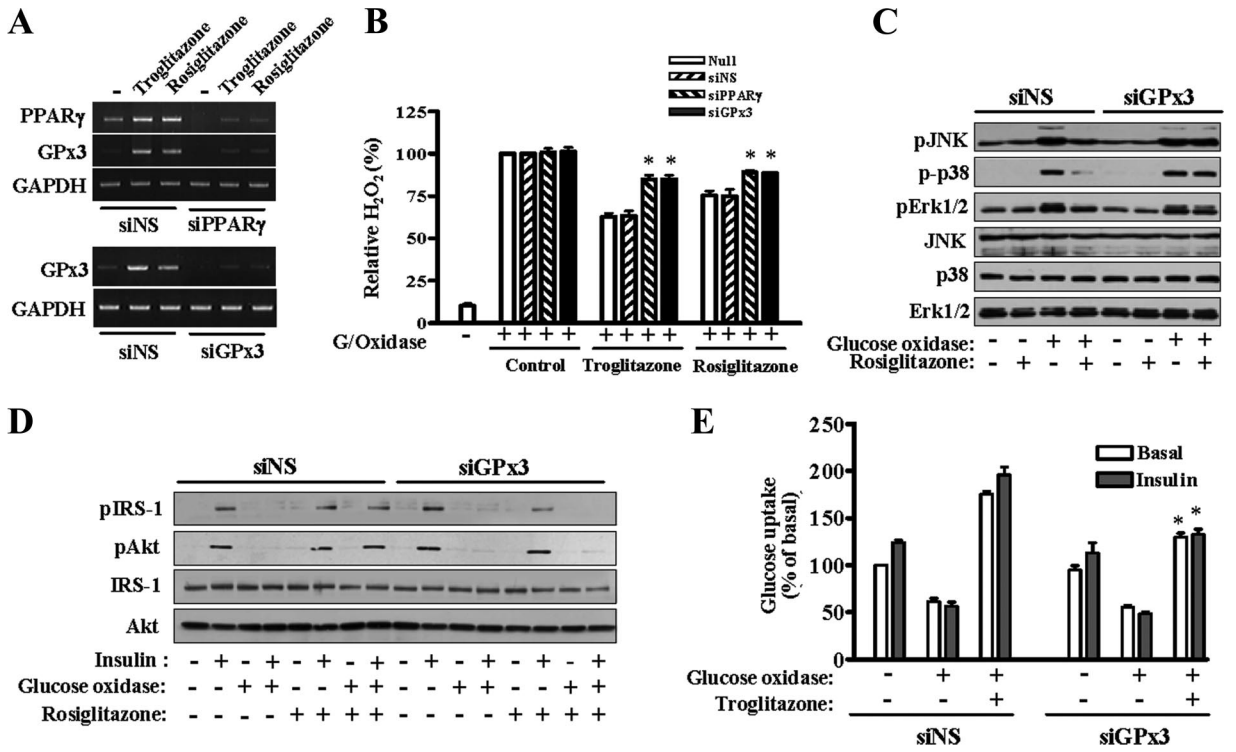

FIG. 7. Effect of GPx3 siRNA on the extracellular H_2O_2 concentration and the insulin signaling pathway. For each panel, at least three independent experiments were performed, and similar results were obtained. (A) Human skeletal muscle cells were transfected with siRNAs of NS (control), PPARγ, or GPx3 for 24 h and then treated with troglitazone or rosiglitazone for an additional 48 h. RNAs were prepared, and the reduction of mRNAs of PPARγ or GPx3 was confirmed by reverse transcription-PCR. (B) The cells were transfected with siRNAs and TZDs as described for panel A. The H_2O_2 level was measured 1 h after treatment with glucose oxidase (G/Oxidase). The bar graph represents the mean ± standard error of five independent experiments. *, $P < 0.01$ versus the value of control (NS) siRNA-treated cells treated in the same way with TZDs. (C) The cells were transfected with siRNAs of NS (siNS) or GPx3 (siGPx3) for 24 h and treated with rosiglitazone for an additional 48 h. The cells were harvested after treatment with glucose oxidase (3 h), and the cellular proteins were subjected to SDS-polyacrylamide gel electrophoresis and Western blot analysis. (D) The cells were treated with siRNAs, rosiglitazone, and glucose oxidase sequentially as described above and then with insulin for 30 min. Western blot analysis was then performed. (E) Glucose uptake was measured using siRNA-treated cells. The value from the cells that had been transfected with NS siRNA and not treated with either glucose oxidase or troglitazone was set as 100, and the other values were shown in relation to it. The bar graph shows the mean ± standard error of five independent experiments. *, $P < 0.05$ versus troglitazone- and glucose oxidase-treated cells of siNS.

for the antioxidant effect of TZDs (Fig. 2), and GPx3 siRNA significantly inhibits the antioxidant effect of TZDs (Fig. 7).

The mitochondrion is a major organelle concerned with the production of ROS in cells, and chronic treatment of glucose and free fatty acids increases the ROS levels in muscle and other tissues (14). In addition, inflammatory cytokines such as tumor necrosis factor alpha (TNF-α) also increase ROS levels and the increased ROS may contribute to the induction of insulin resistance, although other mechanisms are also involved in the induction of insulin resistance by these factors (34). To test whether TZD-mediated GPx3 expression can affect insulin resistance induced by TNF-α, human muscle cells were treated with TNF-α (see Fig. S4 in the supplemental material). As expected, TNF-α treatment impaired the insulin signaling pathway, and rosiglitazone partially alleviated insulin resistance. Interestingly, GPx3 knockdown partially inhibited the effect of rosiglitazone, suggesting an important role of GPx3 in the protective function of TZDs against insulin resistance.

In this study, we showed that the plasma GPx3 level is decreased in newly diagnosed, drug-naive diabetic patients compared to subjects with IGT or NGT. Plasma ROS levels have been reported to be significantly higher in diabetic animals (28); therefore, reduction of plasma GPx3 may be an important reason for the elevation of plasma ROS levels. Several reports illustrate the relationship between GPx3 levels and the pathogenesis of various diseases. Renal GPx3 expression is reduced in long-term diabetic NOD mice but is increased in new-onset diabetic NOD mice (50). Decreased GPx3 levels are associated with arterial thrombosis in ischemic heart disease patients (41) and familial childhood stroke (29). A promoter polymorphism in the GPx3 gene is associated with reduced gene expression and arterial ischemic stroke (48). Plasma GPx3 deficiency impairs normal inhibition of platelet activation by NO, thereby resulting in hyperreactive platelet aggregation (29). These observations suggest that a low level of GPx3 is associated with cardiovascular diseases and diabetes. We also observed that GPx3 expression in the muscle tissues of *db*/*db* mice and high-fat diet-fed mice was lower than that of normal mice. In contrast, little difference was observed between the renal tissues—where GPx3 is most abundantly expressed—obtained from these two groups of mice (data not shown). We are unaware regarding the contribution of each

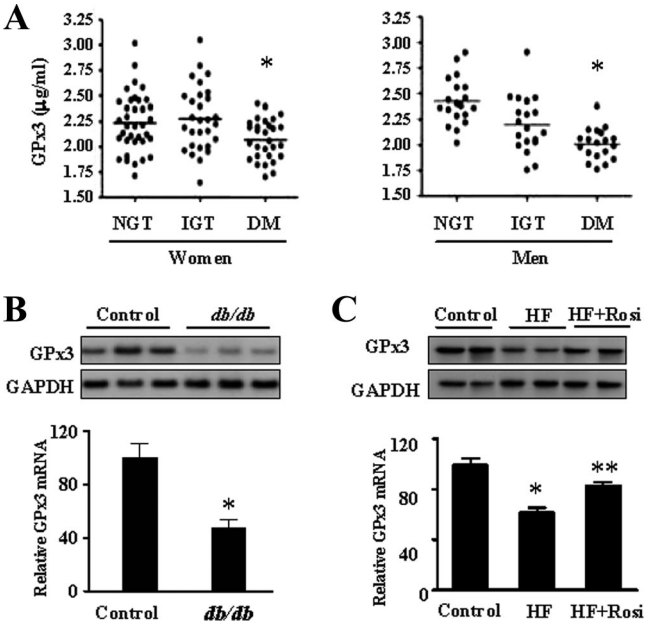

FIG. 8. The expression of GPx3 in diabetic patients and animal models. (A) Plasma GPx3 levels among subjects with NGT ($n = 57$), IGT ($n = 48$), and type 2 DM ($n = 49$) were measured by ELISA. *, $P < 0.01$ versus NGT. (B) Total RNA was prepared from normal or *db*/*db* mouse muscles, and Northern blot analysis was performed using GPx3 and GAPDH probes. The intensity of the GPx3 band was normalized with that of the GAPDH band, and the mean value from the control mice was set as 100. The bar graph represents the mean ± standard error of six normal and six *db*/*db* mice. *, $P < 0.05$. (C) Total RNA was prepared from the skeletal muscle of standard chow-fed (control, $n = 5$), high-fat diet-fed (HF; $n = 5$), and high-fat diet-fed/rosiglitazone-treated (HF + Rosi; $n = 5$) mice, and Northern blot analysis was performed using GPx3 and GAPDH probes. The intensity of the GPx3 band was normalized with that of the GAPDH band, and the mean value from the control mice was set as 100. The bar graph represents the mean ± standard error. *, $P < 0.05$ versus the control mice; **, $P < 0.05$ versus high-fat diet-fed mice.

type of tissue expressing GPx3 to the determination of the plasma GPx3 level; however, it is possible that a reduction in GPx3 expression in the muscle tissue in diabetic subjects can at least influence the oxidative stress around the muscle. The mechanism behind the downregulation of GPx3 in DM is currently unknown. Since GPx3 expression was observed to have decreased in the muscle tissue of type 2 diabetic patients and of *db*/*db* and DIO mice, it may be due to common factors in these insulin-resistant states such as hyperinsulinemia, hyperglycemia, or low-grade inflammation. Recently, we and our coworkers found that in adipose tissue, GPx3 expression is reduced by inflammation or hypoxia (33). Little is known regarding the regulation of GPx3 expression, and therefore, further intensive study is required to elucidate the mechanism by which the GPx3 level is downregulated in DM. In conclusion, the results of this study suggest that GPx3 plays an important role against oxidative stress and may be a therapeutic target for insulin resistance and DM.

ACKNOWLEDGMENT

This study was supported by 21C Frontier Functional Proteomics Project from the Korean Ministry of Education, Science and Technology and MarineBio21, Ministry of Maritime Affairs and Fisheries, South Korea.

REFERENCES

1. **American Diabetes Association.** 2006. Diagnosis and classification of diabetes mellitus. Diabetes Care **29:**S43–S48.
2. **Antunes, F., and E. Cadenas.** 2000. Estimation of H2O2 gradients across biomembranes. FEBS Lett. **475:**121–126.
3. **Berry, M. J., L. Banu, Y. Y. Chen, S. J. Mandel, J. D. Kieffer, J. W. Harney, and P. R. Larsen.** 1991. Recognition of UGA as a selenocysteine codon in type I deiodinase requires sequences in the 3′ untranslated region. Nature **353:**273–276.
4. **Blair, A. S., E. Hajduch, G. J. Litherland, and H. S. Hundal.** 1999. Regulation of glucose transport and glycogen synthesis in L6 muscle cells during oxidative stress. Evidence for cross-talk between the insulin and SAPK2/p38 mitogen-activated protein kinase signaling pathways. J. Biol. Chem. **274:**36293–36299.
5. **Brigelius-Flohe, R.** 1999. Tissue-specific functions of individual glutathione peroxidases. Free Radic. Biol. Med. **27:**951–965.
6. **Brownlee, M.** 2001. Biochemistry and molecular cell biology of diabetic complications. Nature **414:**813–820.
7. **Carlsson, C., L. A. Borg, and N. Welsh.** 1999. Sodium palmitate induces partial mitochondrial uncoupling and reactive oxygen species in rat pancreatic islets in vitro. Endocrinology **140:**3422–3428.
8. **Chu, F. F., R. S. Esworthy, J. H. Doroshow, K. Doan, and X. F. Liu.** 1992. Expression of plasma glutathione peroxidase in human liver in addition to kidney, heart, lung, and breast in humans and rodents. Blood **79:**3233–3238.
9. **Da Ros, R., R. Assaloni, and A. Ceriello.** 2004. The preventive anti-oxidant action of thiazolidinediones: a new therapeutic prospect in diabetes and insulin resistance. Diabet. Med. **21:**1249–1252.
10. **Degenhardt, T., M. Matilainen, K. H. Herzig, T. W. Dunlop, and C. Carlberg.** 2006. The insulin-like growth factor-binding protein 1 gene is a primary target of peroxisome proliferator-activated receptors. J. Biol. Chem. **281:**39607–39619.
11. **Drevet, J. R.** 2006. The antioxidant glutathione peroxidase family and spermatozoa: a complex story. Mol. Cell. Endocrinol. **250:**70–79.
12. **Evans, J. L., I. D. Goldfine, B. A. Maddux, and G. M. Grodsky.** 2002. Oxidative stress and stress-activated signaling pathways: a unifying hypothesis of type 2 diabetes. Endocr. Rev. **23:**599–622.
13. **Ferre, P.** 2004. The biology of peroxisome proliferator-activated receptors: relationship with lipid metabolism and insulin sensitivity. Diabetes **53**(Suppl. 1)**:**S43–S50.
14. **Fridlyand, L. E., and L. H. Philipson.** 2006. Reactive species and early manifestation of insulin resistance in type 2 diabetes. Diabetes Obes. Metab. **8:**136–145.
15. **Furukawa, S., T. Fujita, M. Shimabukuro, M. Iwaki, Y. Yamada, Y. Nakajima, O. Nakayama, M. Makishima, M. Matsuda, and I. Shimomura.** 2004. Increased oxidative stress in obesity and its impact on metabolic syndrome. J. Clin. Investig. **114:**1752–1761.
16. **Gardner, C. D., S. Eguchi, C. M. Reynolds, K. Eguchi, G. D. Frank, and E. D. Motley.** 2003. Hydrogen peroxide inhibits insulin signaling in vascular smooth muscle cells. Exp. Biol. Med. (Maywood) **228:**836–842.
17. **Girnun, G. D., F. E. Domann, S. A. Moore, and M. E. Robbins.** 2002. Identification of a functional peroxisome proliferator-activated receptor response element in the rat catalase promoter. Mol. Endocrinol. **16:**2793–2801.
18. **Giugliano, D., A. Ceriello, and G. Paolisso.** 1995. Diabetes mellitus, hypertension, and cardiovascular disease: which role for oxidative stress? Metabolism **44:**363–368.
19. **Guan, H. P., T. Ishizuka, P. C. Chui, M. Lehrke, and M. A. Lazar.** 2005. Corepressors selectively control the transcriptional activity of PPARgamma in adipocytes. Genes Dev. **19:**453–461.
20. **Haber, C. A., T. K. Lam, Z. Yu, N. Gupta, T. Goh, E. Bogdanovic, A. Giacca, and I. G. Fantus.** 2003. N-acetylcysteine and taurine prevent hyperglycemia-induced insulin resistance in vivo: possible role of oxidative stress. Am. J. Physiol. Endocrinol. Metab. **285:**E744–E753.
21. **Hansen, L. L., Y. Ikeda, G. S. Olsen, A. K. Busch, and L. Mosthaf.** 1999. Insulin signaling is inhibited by micromolar concentrations of H_2O_2. Evidence for a role of H_2O_2 in tumor necrosis factor alpha-mediated insulin resistance. J. Biol. Chem. **274:**25078–25084.
22. **Henry, R. R., L. Abrams, S. Nikoulina, and T. P. Ciaraldi.** 1995. Insulin action and glucose metabolism in nondiabetic control and NIDDM subjects. Comparison using human skeletal muscle cell cultures. Diabetes **44:**936–946.
23. **Hevener, A. L., W. He, Y. Barak, J. Le, G. Bandyopadhyay, P. Olson, J. Wilkes, R. M. Evans, and J. Olefsky.** 2003. Muscle-specific Pparg deletion causes insulin resistance. Nat. Med. **9:**1491–1497.
24. **Hildebrandt, W., A. Hamann, H. Krakowski-Roosen, R. Kinscherf, K. Dugi, R. Sauer, S. Lacher, N. Nobel, A. Bodens, V. Bellou, L. Edler, P. Nawroth, and W. Droge.** 2004. Effect of thiol antioxidant on body fat and insulin reactivity. J. Mol. Med. **82:**336–344.
25. **Hong, H. K., Y. M. Cho, K. H. Park, C. T. Lee, H. K. Lee, and K. S. Park.** 2003. Peroxisome proliferator-activated receptor gamma mediated inhibi-

tion of plasminogen activator inhibitor type 1 production and proliferation of human umbilical vein endothelial cells. Diabetes Res. Clin. Pract. **62:**1–8.
26. **Houstis, N., E. D. Rosen, and E. S. Lander.** 2006. Reactive oxygen species have a causal role in multiple forms of insulin resistance. Nature **440:**944–948.
27. **Inoue, I., S. Goto, T. Matsunaga, T. Nakajima, T. Awata, S. Hokari, T. Komoda, and S. Katayama.** 2001. The ligands/activators for peroxisome proliferator-activated receptor alpha (PPARalpha) and PPARgamma increase Cu^{2+},Zn^{2+}-superoxide dismutase and decrease p22phox message expressions in primary endothelial cells. Metabolism **50:**3–11.
28. **Karasu, C.** 2000. Time course of changes in endothelium-dependent and -independent relaxation of chronically diabetic aorta: role of reactive oxygen species. Eur. J. Pharmacol. **392:**163–173.
29. **Kenet, G., J. Freedman, B. Shenkman, E. Regina, F. Brok-Simoni, F. Holzman, F. Vavva, N. Brand, A. Michelson, M. Trolliet, J. Loscalzo, and A. Inbal.** 1999. Plasma glutathione peroxidase deficiency and platelet insensitivity to nitric oxide in children with familial stroke. Arterioscler. Thromb. Vasc. Biol. **19:**2017–2023.
30. **Kryukov, G. V., S. Castellano, S. V. Novoselov, A. V. Lobanov, O. Zehtab, R. Guigo, and V. N. Gladyshev.** 2003. Characterization of mammalian selenoproteomes. Science **300:**1439–1443.
31. **Kyriakis, J. M., and J. Avruch.** 1996. Sounding the alarm: protein kinase cascades activated by stress and inflammation. J. Biol. Chem. **271:**24313–24316.
32. **Lee, K. S., S. R. Kim, S. J. Park, H. S. Park, K. H. Min, S. M. Jin, M. K. Lee, U. H. Kim, and Y. C. Lee.** 2006. Peroxisome proliferator activated receptor-gamma modulates reactive oxygen species generation and activation of nuclear factor-kappaB and hypoxia-inducible factor 1alpha in allergic airway disease of mice. J. Allergy Clin. Immunol. **118:**120–127.
33. **Lee, Y. S., A. Y. Kim, J. W. Choi, M. Kim, S. Yasue, H. J. Son, H. Masuzaki, K. S. Park, and J. B. Kim.** 2008. Dysregulation of adipose glutathione peroxidase 3 in obesity contributes to local and systemic oxidative stress. Mol. Endocrinol. **22:**2176–2189.
34. **Lorenzo, M., S. Fernandez-Veledo, R. Vila-Bedmar, L. Garcia-Guerra, C. De Alvaro, and I. Nieto-Vazquez.** 2008. Insulin resistance induced by tumor necrosis factor-alpha in myocytes and brown adipocytes. J. Anim. Sci. **86:** E94–E104.
35. **Maddipati, K. R., and L. J. Marnett.** 1987. Characterization of the major hydroperoxide-reducing activity of human plasma. Purification and properties of a selenium-dependent glutathione peroxidase. J. Biol. Chem. **262:** 17398–17403.
36. **Maddux, B. A., W. See, J. C. Lawrence, Jr., A. L. Goldfine, I. D. Goldfine, and J. L. Evans.** 2001. Protection against oxidative stress-induced insulin resistance in rat L6 muscle cells by micromolar concentrations of alpha-lipoic acid. Diabetes **50:**404–410.
37. **Maeda, K., K. Okubo, I. Shimomura, K. Mizuno, Y. Matsuzawa, and K. Matsubara.** 1997. Analysis of an expression profile of genes in the human adipose tissue. Gene **190:**227–235.
38. **Maglara, A. A., A. Vasilaki, M. J. Jackson, and A. McArdle.** 2003. Damage to developing mouse skeletal muscle myotubes in culture: protective effect of heat shock proteins. J. Physiol. **548:**837–846.
39. **Maser, R. L., B. S. Magenheimer, and J. P. Calvet.** 1994. Mouse plasma glutathione peroxidase. cDNA sequence analysis and renal proximal tubular expression and secretion. J. Biol. Chem. **269:**27066–27073.
40. **Park, K. S., J. H. Kim, M. S. Kim, J. M. Kim, S. K. Kim, J. Y. Choi, M. H. Chung, B. Han, S. Y. Kim, and H. K. Lee.** 2001. Effects of insulin and antioxidant on plasma 8-hydroxyguanine and tissue 8-hydroxydeoxyguanosine in streptozotocin-induced diabetic rats. Diabetes **50:**2837–2841.
41. **Porter, M., D. J. Pearson, V. J. Suarez-Mendez, and A. D. Blann.** 1992. Plasma, platelet and erythrocyte glutathione peroxidases as risk factors in ischaemic heart disease in man. Clin. Sci. (London) **83:**343–345.
42. **Rosen, E. D., C. J. Walkey, P. Puigserver, and B. M. Spiegelman.** 2000. Transcriptional regulation of adipogenesis. Genes Dev. **14:**1293–1307.
43. **Shin, C. S., B. S. Moon, K. S. Park, S. Y. Kim, S. J. Park, M. H. Chung, and H. K. Lee.** 2001. Serum 8-hydroxy-guanine levels are increased in diabetic patients. Diabetes Care **24:**733–737.
44. **Takebe, G., J. Yarimizu, Y. Saito, T. Hayashi, H. Nakamura, J. Yodoi, S. Nagasawa, and K. Takahashi.** 2002. A comparative study on the hydroperoxide and thiol specificity of the glutathione peroxidase family and selenoprotein P. J. Biol. Chem. **277:**41254–41258.
45. **Tirosh, A., R. Potashnik, N. Bashan, and A. Rudich.** 1999. Oxidative stress disrupts insulin-induced cellular redistribution of insulin receptor substrate-1 and phosphatidylinositol 3-kinase in 3T3-L1 adipocytes. A putative cellular mechanism for impaired protein kinase B activation and GLUT4 translocation. J. Biol. Chem. **274:**10595–10602.
46. **Tontonoz, P., E. Hu, and B. M. Spiegelman.** 1994. Stimulation of adipogenesis in fibroblasts by PPAR gamma 2, a lipid-activated transcription factor. Cell **79:**1147–1156.
47. **Urakawa, H., A. Katsuki, Y. Sumida, E. C. Gabazza, S. Murashima, K. Morioka, N. Maruyama, N. Kitagawa, T. Tanaka, Y. Hori, K. Nakatani, Y. Yano, and Y. Adachi.** 2003. Oxidative stress is associated with adiposity and insulin resistance in men. J. Clin. Endocrinol. Metab. **88:**4673–4676.
48. **Voetsch, B., R. C. Jin, C. Bierl, K. S. Benke, G. Kenet, P. Simioni, F. Ottaviano, B. P. Damasceno, J. M. Annichino-Bizacchi, D. E. Handy, and J. Loscalzo.** 2007. Promoter polymorphisms in the plasma glutathione peroxidase (GPx-3) gene: a novel risk factor for arterial ischemic stroke among young adults and children. Stroke **38:**41–49.
49. **West, I. C.** 2000. Radicals and oxidative stress in diabetes. Diabet. Med. **17:**171–180.
50. **Wilson, K. H., S. E. Eckenrode, Q. Z. Li, Q. G. Ruan, P. Yang, J. D. Shi, A. Davoodi-Semiromi, R. A. McIndoe, B. P. Croker, and J. X. She.** 2003. Microarray analysis of gene expression in the kidneys of new- and post-onset diabetic NOD mice. Diabetes **52:**2151–2159.
51. **Yamamoto, Y., and K. Takahashi.** 1993. Glutathione peroxidase isolated from plasma reduces phospholipid hydroperoxides. Arch. Biochem. Biophys. **305:**541–545.
52. **Yoshimura, S., K. Watanabe, H. Suemizu, T. Onozawa, J. Mizoguchi, K. Tsuda, H. Hatta, and T. Moriuchi.** 1991. Tissue specific expression of the plasma glutathione peroxidase gene in rat kidney. J. Biochem. (Tokyo) **109:**918–923.